



Temporal investigation of effects of wildfires and aerosols on air pollution changes in Nigeria: a multivariate modelling approach

Tertsea Igbawua*

Department of Physics, Joseph Sarwuan Tarka University, Makurdi

ARTICLE INFO

Article history:

Received: 11 May 2025

Received in revised form: 16 November 2025

Accepted: 17 November 2025

Available online: 26 December 2025

Keywords: AOD, Wildfires, Multivariate regression, Black carbon, Sea salt

DOI: 10.61298/rans.2025.3.2.212

ABSTRACT

Understanding the factors that influence Aerosol Optical Depth (AOD) is essential for addressing air pollution and effectively managing air quality. This study examines the impacts of dust aerosol (DU), sea salt (SS), black carbon (BC), and burned areas (BA) on AOD across different Köppen climate zones in Nigeria from 2001 to 2019. Results from a multivariate regression analysis revealed that DU consistently had a strong and significant impact on AOD across all zones (coefficients: between 0.00106 and 0.00779, $p < 0.001$), indicating the influence of dust from the Sahara Desert and the Bodélé Depression. BC and SS increased AOD in southern and coastal zones, although BC had a negative impact in Aw climate zones. The influence of BC was less consistent, indicating its varied sources, including gas flaring and urban emissions. BA showed mixed effects on AOD across different climate zones. In some zones, BA had a positive but often insignificant impact on AOD, while in others, it exhibited negligible or negative coefficients. This suggests that although biomass burning contributes to aerosol levels, its direct effect on AOD may be mitigated by factors such as precipitation and aerosol interactions during the burning season. SS generally had a significant positive relationship with AOD. Peaks in SS levels in the mid-2000s and mid-2010s correlated with higher AOD, emphasizing the maritime influence on aerosol levels in these regions. However, the impact of SS on AOD was less pronounced in the BWh zone, reflecting regional differences in aerosol composition and sources. These findings demonstrate the major impact of dust aerosols and the complex contributions of other sources, offering insights for climate-sensitive air quality management in Nigeria.

© 2025 The Author(s). Production and Hosting by FLAYOO Publishing House LTD on Behalf of the Nigerian Society of Physical Sciences (NSPS). Peer review under the responsibility of NSPS. This is an open access article under the terms of the [Creative Commons Attribution 4.0 International license](https://creativecommons.org/licenses/by/4.0/). Further distribution of this work must maintain attribution to the author(s) and the published article's title, journal citation, and DOI.

1. INTRODUCTION

Black Carbon (BC) emissions significantly impact air quality and climate, originating from various anthropogenic sources such

as vehicular emissions, industrial processes, domestic activities, and wildfires [1, 2]. BC, a short-lived climate forcer, has localized effects due to its relatively brief atmospheric lifetime [3]. It is a major component of combustion aerosols, alongside organic carbon (OC); BC primarily absorbs solar radiation, whereas OC mainly scatters it [4]. Biomass burning from forest fires, driven

*Corresponding author Tel. No.: +234-803-6952-266

e-mail: tertsea.igbawua@uam.edu.ng (Tertsea Igbawua)

by both natural and human activities, exacerbates environmental degradation and poses substantial public health risks [2, 5].

In Africa, BC emissions from sub-Saharan regions are known to influence regional climate and public health. However, limited ground-based data and uncertain emission sources present challenges to fully understanding these impacts [6]. The substantial burned area (BA) in sub-Saharan Africa, often underestimated in coarse-resolution datasets, significantly contributes to global carbon emissions [7]. Various methods, including global atmospheric models and satellite observations, are used to study BC's transport and dispersion, indicating its far-reaching effects [8–10].

In Nigeria, air pollution primarily originates from desert dust, black carbon emitted by gas flares, and biomass combustion [11]. Studies show that emissions from biomass burning in Central Africa affect air quality in cities along the Gulf of Guinea, with pollutants being transported and vertically mixed, thereby influencing regional atmospheric conditions [12]. Seasonal variations and meteorological phenomena, such as the Intertropical Convergence Zone (ITCZ), play a crucial role in regulating aerosol optical depth (AOD) across Nigeria's diverse ecological zones [13]. According to Atai *et al.* [14], seasonal fluctuations in Saharan Africa are associated with changes in AOD and the Bodélé Depression in Chad, which contributes approximately 40% of the region's dust (DU), particularly during the harmattan season.

Unlike earlier AOD studies in Nigeria that primarily focused on seasonal variations, meteorological effects, or dataset comparisons [15–18], this study advances the field by integrating multiple datasets to analyze the combined impacts of natural and anthropogenic activities on aerosol loadings. While previous research has emphasized the influence of humidity, wind, and the intertropical discontinuity in shaping AOD patterns [13, 15], our study investigates how wildfire activity (BA) and different aerosol types (e.g., DU, BC, and SS) interact within various Köppen climate zones in Nigeria. By linking AOD variability to wildfire emissions and broader atmospheric processes, this work provides a more comprehensive spatial and temporal understanding of aerosol variations across climate zones.

Given the significant role of aerosols in influencing climate, hydrological processes, and ecosystems, this study aims to evaluate the temporal impacts of wildfires and aerosols on air pollution changes in Nigeria. Using a multivariate modeling approach, the work examines the relationship between AOD and key factors such as BA, BC, DU, and SS, to enhance our understanding of air pollution dynamics and inform mitigation strategies in Nigeria.

2. METHODOLOGY

2.1. STUDY AREA

Nigeria, located in sub-Saharan Africa, is a diverse country situated between the Sahara Desert to the north and the Atlantic Ocean to the south. It comprises 36 states and the Federal Capital Territory (FCT). The country features a variety of climate zones, as classified by the Köppen climate classification system (see Figure 1).

In the southern region, Nigeria has a tropical rainforest climate (Af), characterized by heavy rainfall and dense vegetation. Moving slightly northward, the tropical monsoon climate (Am) predominates, with a short dry season, along with generally high

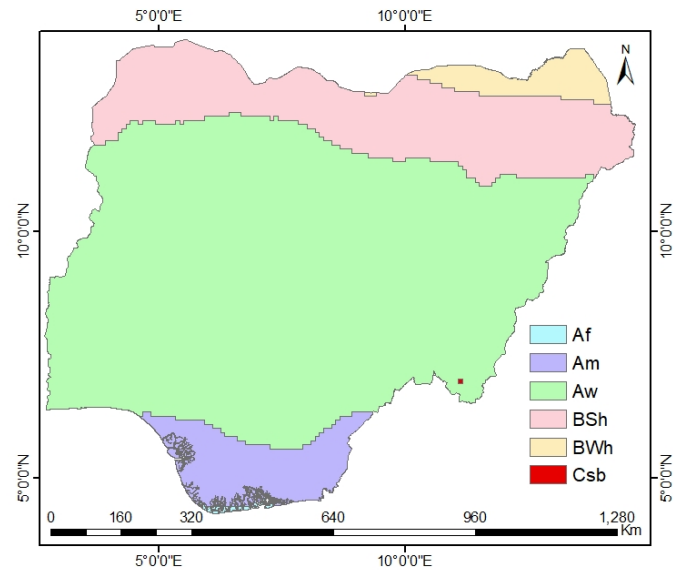


Figure 1. Study area with Köppen climate classification.

humidity and precipitation. The central part of Nigeria primarily experiences a tropical savanna climate (Aw), where distinct wet and dry seasons shape the landscape and weather patterns. The northern regions experience semi-arid (BSh) and arid (BWh) climates, which significantly contribute to dust aerosol emissions, particularly due to their proximity to the Sahara Desert.

Additionally, the southern coastal areas, influenced by the Atlantic Ocean, are sources of sea salt aerosols. The Csb climate zone (Mediterranean with warm summers) occurs in small regions across Nigeria. The country's rapidly growing population participates in various activities that contribute to biomass burning, a major source of air pollution. Moreover, wildfires are widespread throughout Nigeria, many of which are intentionally set by humans. These fires, combined with other pollution sources, significantly affect air quality and environmental conditions across the country.

2.2. DATA

The burned areas depicting wildfires were obtained from the Copernicus Climate Change Service [19]. AOD [20] and other aerosol variables BC, DU, and SS [21] were sourced from the Modern-Era Retrospective Analysis for Research and Applications, Version 2 (MERRA-2). The MERRA-2 datasets were re-sampled to match the resolution of the burned area data, which is available only from 2001 to 2019. The Köppen climate classification, as provided by Beck *et al.* [22], was used to offer a qualitative framework for describing the climates of specific regions within the study area. This data was accessed from <https://www.gloh2o.org/koppen/>. A summary of the datasets is presented in Table 1.

2.3. METHODOLOGY

2.3.1. Data extraction and data processing

The Köppen climate classification was used to divide the study area into distinct climate zones, enabling a more detailed analysis of the data. The specific climate zones included in the analysis

Table 1. Data summary.

S/N	Data	Source	Resolution	Span
1	Burned Area (Km ²)	CDS	0.25° × 0.25°	2001 - 2019
2	Black Carbon (μg/m ³)	MERRA2	0.50° × 0.625°	2001 - 2019
3	Dust (μg/m ³)	MERRA2	0.50° × 0.625°	2001 - 2019
4	Sea salt (μg/m ³)	MERRA2	0.50° × 0.625°	2001 - 2019
5	AOD	MERRA2	0.50° × 0.625°	2001 - 2019
6	Koppen			

were Af, Am, Aw, BSh, BWh, and Csb. Data for AOD, BA, BC, DU, and SS were extracted for each Köppen climate zone. AOD was treated as the dependent variable, while BA, BC, DU, and SS served as independent variables. The dataset was split into training and testing sets, with 70% used to train the model and the remaining 30% reserved for testing.

2.3.2. Multivariate regression model

A multivariate regression model was employed to analyze the relationship between AOD and the independent variables (BA, BC, DU, and SS). The model [23, 24] is expressed as:

$$AOD = \beta_o + \beta_1 BA + \beta_2 BC + \beta_3 DU + \beta_4 SS + \varepsilon, \quad (1)$$

where AOD is the dependent variable, β_o is the intercept, $\beta_1, \beta_2, \beta_3,$ and β_4 are the coefficients for the independent variables BA, BC, DU, and SS, respectively. The error term is represented by ε .

2.3.3. Model training and testing

The model was implemented in R, a statistical computing language. The training set (70% of the data) was used to estimate the coefficients of the regression model. The model's performance was evaluated on the test set (30% of the data) using the R-squared metric to measure goodness of fit [25]. The R-squared value was calculated to assess how well the model explains the variability of the dependent variable (AOD). The R-squared value ranges from 0 to 1, with values closer to 1 indicating a better fit.

$$R^2 = 1 - \frac{\sum_{i=1}^n (x_i - \hat{y}_i)^2}{\sum_{i=1}^n (x_i - \bar{y}_i)^2}, \quad (2)$$

where x_i is the observed value, \hat{y}_i is the predicted value, and \bar{y}_i is the mean of the observed values, and n is the number of observations.

3. RESULTS

3.1. SPATIAL DISTRIBUTION OF AOD AND AEROSOL VARIABLES IN NIGERIA

Figure 2 illustrates the spatial distribution of mean AOD, DU, BA, BC, and SS variables across Nigeria from 2001 to 2019. The spatial patterns of these aerosol-related parameters reveal distinct regional variations. AOD values peak in the southwest, parts of the northcentral, and northwest regions, indicating high aerosol concentrations. In contrast, the central, south-south, and southeastern regions exhibit moderate levels, while the Mambila and Jos plateaus show the lowest values. Dust concentrations are

highest in the northern regions, particularly the northeast, due to the influence of the Sahara Desert, whereas the southern regions experience minimal dust. Burned areas are concentrated in the central belt and northern regions, reflecting significant biomass burning activities, while the southernmost regions have fewer fires. Black carbon concentrations are highest in the southern regions, especially the southwest, likely due to urban and industrial activities, with lower levels observed in the north. Sea salt concentrations are highest along the southern coastal areas, influenced by the Atlantic Ocean, and decrease sharply inland.

3.2. TEMPORAL DISTRIBUTION OF AOD AND AEROSOL VARIABLES IN NIGERIA

Figure 3 illustrates the changes in AOD and related variables across Nigeria from 2001 to 2019, showing significant variability among different Köppen climate zones. The Af and Am zones exhibit noticeable peaks in AOD in 2004, 2008, and 2016, followed by a decline toward 2019. The Aw zone peaks in 2005 and 2017, with marked decreases around 2010 and 2014. The BSh and BWh zones are more stable, although the BWh zone shows a slight upward trend, with highs in 2002, 2008, and 2017, and lows in 2003, 2010, and 2014. The Csb zone fluctuates erratically, peaking in 2002, 2003, and 2017, and dropping in 2010, 2013, and 2014.

Figure 3b highlights significant fluctuations in DU levels across various climate zones in Nigeria from 2001 to 2019. The Af and Am zones show notable variability, with peaks around 2004, 2008, 2015, and 2017, and substantial declines in 2003, 2010, and 2019. The Aw zone also exhibits peaks in 2007, 2008, 2015, and 2017, with marked decreases in 2010, 2013, and 2019. The BSh and BWh zones generally have higher DU values, peaking in 2002, 2007, 2015, and 2017, and decreasing in 2003, 2010, 2013, and 2019. The Csb zone experiences wide fluctuations, with peaks in 2004, 2008, 2015, and 2017, and significant drops in 2010, 2013, 2014, and 2019. There is a general downward trend in DU from 2017 to 2019 across most zones, indicating a recent decrease in dust concentration levels.

From 2001 to 2019 (Figure 3c), the SS levels in the Af and Am zones show an overall increase, with notable peaks in 2005, 2015, and 2016, and periodic declines in 2008 and 2011. The Aw zone exhibits a peak in 2005, followed by relatively stable but lower levels in subsequent years, except for a spike in 2016. The BSh and BWh zones maintain generally low SS values with minor fluctuations, showing slight increases around 2007, 2010, and 2016. The Csb zone experiences significant rises in SS levels in 2005, 2007, and particularly in 2015 and 2016, indicating greater variability compared to other zones. Across all zones, SS levels generally peak around the mid-2000s and mid-2010s, with some decline toward the end of the period.

From 2001 to 2019 (Figure 3d), BC levels across the Am and Aw zones exhibit greater variability, with noticeable increases in 2005 and 2007, followed by periods of relative stability or slight decline. The BSh and BWh zones also demonstrate a general upward trend, with peaks in 2010 and a consistent presence of BC throughout the period, indicating persistent emission sources. The Csb zone, however, shows a notable peak in 2005 followed by a decline, reaching its lowest levels in 2014. On the whole, BC levels fluctuate annually across all zones, with certain years,

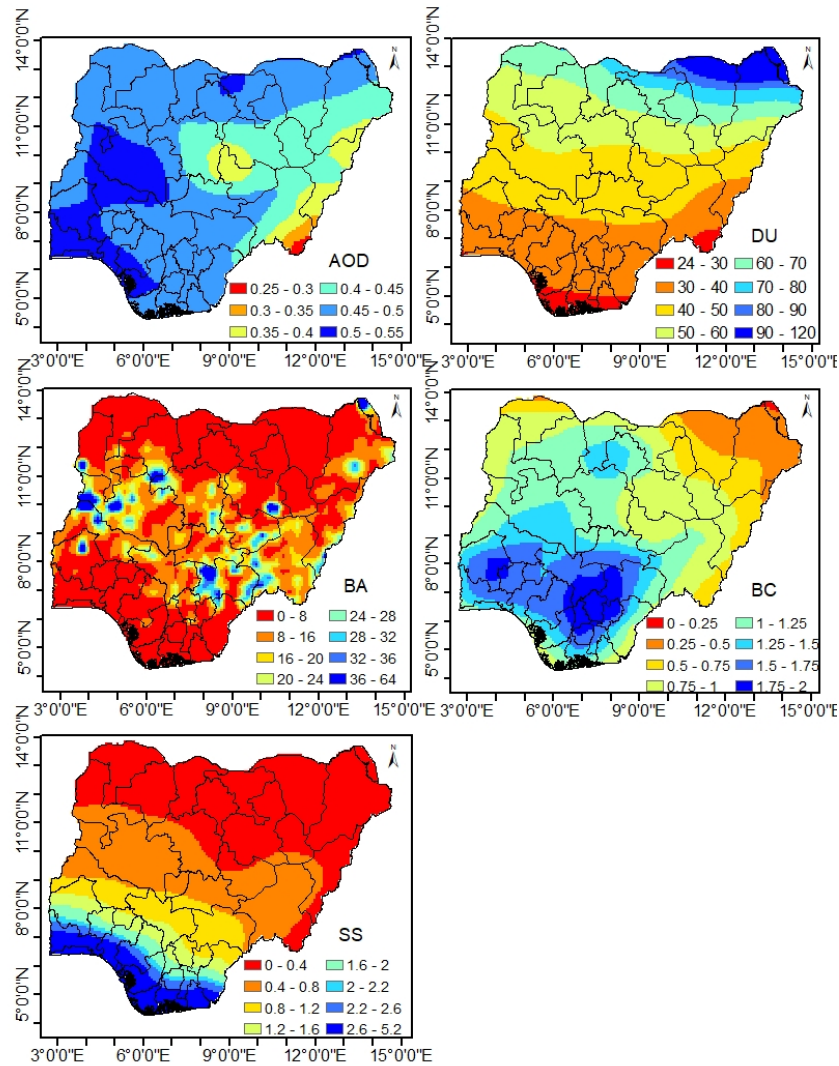


Figure 2. Mean spatial AOD, dust, burned area, black carbon, and sea salt over Nigeria.

such as 2005, standing out due to higher concentrations across most regions, suggesting potential regional or global events influencing these spikes.

Figure 3e shows that from 2001 to 2019, BA in the Af zone peaked in 2007 and 2018, with values exceeding 0.40 km^2 . The Am zone experienced substantial increases in BA, particularly in 2007 and 2016, with additional spikes in 2002 and 2011. The Aw zone consistently recorded the highest BA, reaching over 14.00 km^2 in 2004, although there has been a noticeable decline in recent years, with lower values in 2017 and 2019. The BSh and BWh zones also exhibited high variability, with significant peaks in 2015, 2016, and 2018 for BSh, and in 2005 and 2016 for BWh. The Csb zone experienced considerable fluctuations, with high burned areas in 2005, 2007, and 2016. The data suggest periodic spikes in burned areas, potentially linked to climatic and environmental conditions or human activities influencing fire incidence across these regions.

3.3. MONTHLY DISTRIBUTION OF AOD AND AEROSOL VARIABLES IN NIGERIA

Figure 4 presents the monthly distribution of aerosol variables, including BA and AOD, across Nigeria. The AOD distribution varies among Nigeria's different climatic zones, as illustrated in Figure 4a. Most zones exhibit peak values in February and minimum values in September. In the Af climate, the AOD reaches a maximum of 0.913 in February and drops to a low of 0.176 in September. A similar pattern is observed in the Am climate, with a peak of 0.9601 in February and a low of 0.175 in September. The Aw climate shows a distinct pattern, with an AOD value of 0.240211 in August and a maximum of 0.805 in March. In the BSh and BWh climates, AOD levels are higher in March and lower in August. For the Csb climate, the highest AOD value occurs in March (0.678), while the lowest is in August (0.150).

In Figure 4b, dust aerosol levels vary across different climate zones in Nigeria. For most zones, the highest values occur in January and February. The Af climate peaks at $75.51 \mu\text{g}/\text{m}^3$ in January and reaches a low of $1.06 \mu\text{g}/\text{m}^3$ in August. The Am climate experiences its highest levels in January ($80.05 \mu\text{g}/\text{m}^3$)

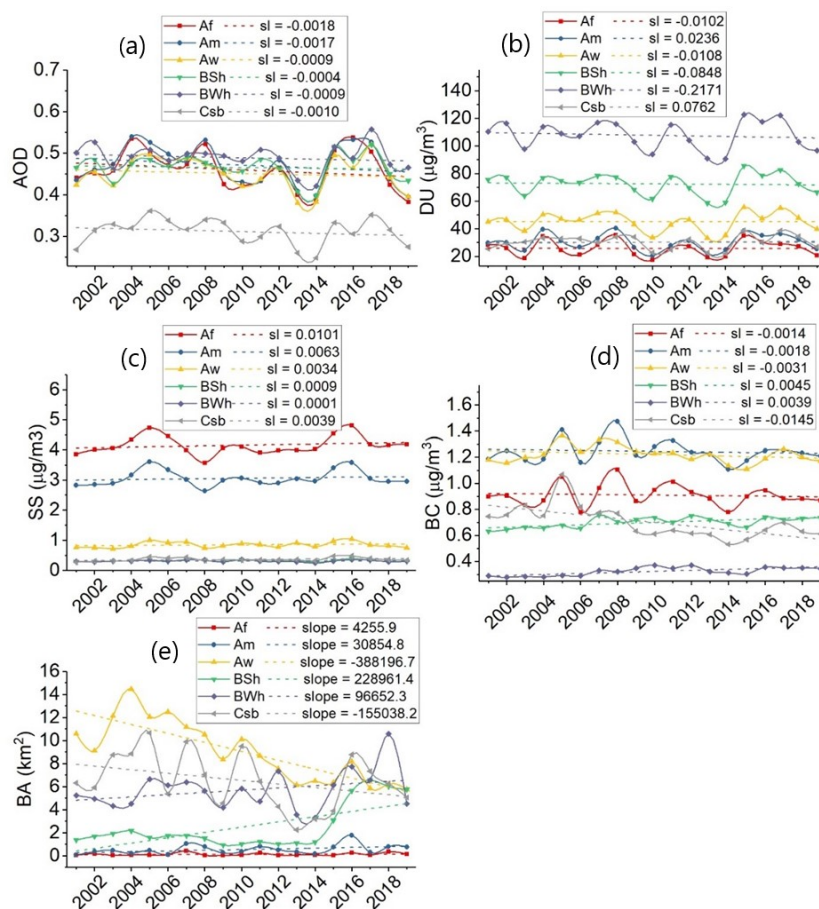


Figure 3. Annual distribution of AOD, BA, and aerosol species (BC, DU, and SS) across Nigeria. The slope (sl) values represent the annual rate of change for each variable. All variables are expressed in consistent units: AOD (unitless), BA (km^2), and aerosol species ($\mu\text{g}/\text{m}^3$).

and February ($87.42 \mu\text{g}/\text{m}^3$), with a minimum in August ($1.33 \mu\text{g}/\text{m}^3$). The Aw climate shows elevated dust levels in January ($87.84 \mu\text{g}/\text{m}^3$) and February ($100.16 \mu\text{g}/\text{m}^3$), with the lowest values in July ($7.84 \mu\text{g}/\text{m}^3$) and August ($6.45 \mu\text{g}/\text{m}^3$). In the BSh climate, DU concentrations are high in January ($130.10 \mu\text{g}/\text{m}^3$) and February ($129.50 \mu\text{g}/\text{m}^3$), and lowest in July ($18.11 \mu\text{g}/\text{m}^3$) and August ($15.27 \mu\text{g}/\text{m}^3$). The BWh climate peaks in January ($190.06 \mu\text{g}/\text{m}^3$) and February ($186.23 \mu\text{g}/\text{m}^3$), with the lowest levels in July ($29.45 \mu\text{g}/\text{m}^3$) and August ($20.84 \mu\text{g}/\text{m}^3$). For the Csb climate zone, the highest DU levels were observed in January ($45.03 \mu\text{g}/\text{m}^3$) and February ($76.95 \mu\text{g}/\text{m}^3$), with the lowest in July ($5.45 \mu\text{g}/\text{m}^3$) and August ($3.45 \mu\text{g}/\text{m}^3$).

In Figure 4c, SS aerosol levels vary across different climate zones in Nigeria. In June, most zones exhibit their highest values, while in December, most zones record their lowest values. In the Af zone, SS aerosol peaks in June ($5.22 \mu\text{g}/\text{m}^3$) and declines to its lowest level in December ($2.91 \mu\text{g}/\text{m}^3$). The Am climate experiences the highest levels in June ($3.86 \mu\text{g}/\text{m}^3$) and the lowest in December ($1.93 \mu\text{g}/\text{m}^3$). The Aw climate shows elevated SS levels in February ($1.20 \mu\text{g}/\text{m}^3$) and the lowest in December ($0.53 \mu\text{g}/\text{m}^3$). The BSh climate displays increased SS concentrations in June ($0.35 \mu\text{g}/\text{m}^3$) and July ($0.31 \mu\text{g}/\text{m}^3$), with the lowest values in January ($0.27 \mu\text{g}/\text{m}^3$) and February ($0.28 \mu\text{g}/\text{m}^3$). The BWh climate reaches its peak in July ($0.41 \mu\text{g}/\text{m}^3$) and its lowest point

in March ($0.25 \mu\text{g}/\text{m}^3$). The Csb climate records the highest SS aerosol levels in March ($0.77 \mu\text{g}/\text{m}^3$) and the lowest in May ($0.29 \mu\text{g}/\text{m}^3$).

In Figure 4d, BC levels vary across different climate zones in Nigeria. For most zones, the highest values occur in January and December. In the Af zone, BC levels peak in January ($2.51 \mu\text{g}/\text{m}^3$) and December ($1.86 \mu\text{g}/\text{m}^3$), with a notable drop in March ($0.55 \mu\text{g}/\text{m}^3$). The Am climate experiences its highest concentrations in January ($3.16 \mu\text{g}/\text{m}^3$) and December ($2.41 \mu\text{g}/\text{m}^3$), with the lowest in February ($1.54 \mu\text{g}/\text{m}^3$). The Aw climate shows elevated BC levels in January ($2.29 \mu\text{g}/\text{m}^3$) and November ($1.41 \mu\text{g}/\text{m}^3$), with a slight dip in February ($1.47 \mu\text{g}/\text{m}^3$). The BSh climate has elevated levels in January ($0.58 \mu\text{g}/\text{m}^3$) and remains relatively high throughout the year, peaking in September ($0.87 \mu\text{g}/\text{m}^3$). The BWh climate exhibits its highest levels in January ($0.18 \mu\text{g}/\text{m}^3$) and peaks again in September ($0.53 \mu\text{g}/\text{m}^3$), with a low in March ($0.16 \mu\text{g}/\text{m}^3$). The Csb climate shows elevated BC levels in December ($1.78 \mu\text{g}/\text{m}^3$) and January ($1.68 \mu\text{g}/\text{m}^3$), with a low in March ($0.63 \mu\text{g}/\text{m}^3$).

In Figure 4e, BA varies across different climate zones in Nigeria. For most zones, the highest values occur in December and January. The Af climate shows the greatest BA in December (0.96 km^2) and January (0.34 km^2), with minimal to no burning from June to September. The Am climate peaks in January (4.23

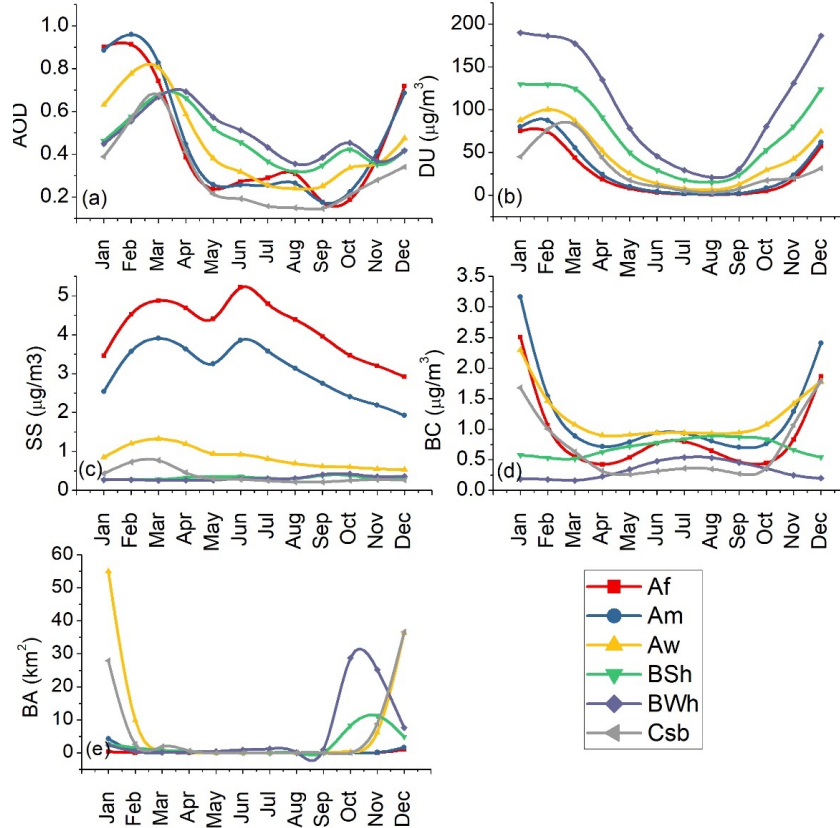


Figure 4. Monthly distribution of AOD, BA, and aerosol variables (BC, DU, and SS) in Nigeria.

km²) and has a notable value in December (1.58 km²), with minimal burning during the mid-year months. In the Aw zone, the maximum BA is observed in January (55.02 km²) and December (36.42 km²), with significantly lower values in the middle of the year. The BSh climate peaks in November (11.23 km²) and October (8.21 km²), with low to no burning during the summer months. The BWh climate experiences its highest BA in October (28.77 km²) and November (25.16 km²), with minimal activity mid-year. The Csb climate has the highest BA values in December (36.61 km²) and January (27.94 km²), with no recorded burning from May to August and in October.

3.4. MULTIVARIATE REGRESSION BETWEEN AOD VERSUS BURNED AREA, BLACK CARBON, SEA SALT, AND DUST

Table 2 presents the multivariate regression analysis of AOD in relation to BA, BC, SS, and DU. The results indicate that in the Af zone, AOD has a significant positive relationship with BC, with a coefficient of 5.29×10^{-2} . Burned Areas (BA) and Sea Salt (SS) also show positive coefficients with AOD (2.64×10^{-8} and 5.54×10^{-2} , respectively), although the coefficient for BA is not statistically significant ($p = 0.272$). Additionally, AOD versus Dust Aerosol (DU) has a coefficient of 7.79×10^{-3} , indicating a strong positive influence on air pollution in the Af zone.

In the Am zone, BC again displays a significant positive coefficient (6.25×10^{-2} , $p = 0.0001$), indicating a substantial influence on AOD. Burned Areas (BA) show a negative coefficient (-8.84×10^{-9}), suggesting a potential decrease in AOD, although this effect is not significant ($p = 0.1309$). DU and SS both ex-

hibit positive coefficients (0.0074 and 0.0741, respectively) with strong significance, demonstrating their impact on AOD in the Am zone.

In the Aw zone, the intercept is notably positive (0.143), indicating a generally higher baseline AOD impact. Black Carbon (BC) shows a significant negative coefficient (-5.33×10^{-2} , $p < 0.05$), suggesting a decrease in AOD impact associated with BC. Burned Areas (BA) have a negligible coefficient (1.94×10^{-10} , $p = 0.7086$), while DU and SS both display positive coefficients (5.58×10^{-3} and 1.47×10^{-1} , respectively), with SS having the greatest impact.

For the BSh zone, the intercept is positive (0.148), suggesting a baseline impact on AOD. BC and SS show significant positive coefficients (4.70×10^{-2} and 4.46×10^{-1} , respectively), indicating their substantial influence on AOD. BA and DU exhibit significant negative and positive coefficients (-6.92×10^{-9} and 2.21×10^{-3} , respectively), revealing their roles in AOD dynamics.

In the BWh zone, the intercept is significantly positive (0.388), indicating a higher baseline impact on AOD compared to other zones. Both BC and BA exhibited significant coefficients, with BC showing a positive coefficient (4.26×10^{-2}) and BA a negative coefficient (-3.76×10^{-9}), suggesting their influence on AOD. DU showed a significant positive coefficient (1.06×10^{-3}), whereas SS exhibited an insignificant negative coefficient (-1.45×10^{-2}).

Lastly, in the Csb zone, the intercept is significantly positive (0.092), indicating a baseline AOD. BC exhibits a significant positive coefficient of 0.0468, demonstrating its influence

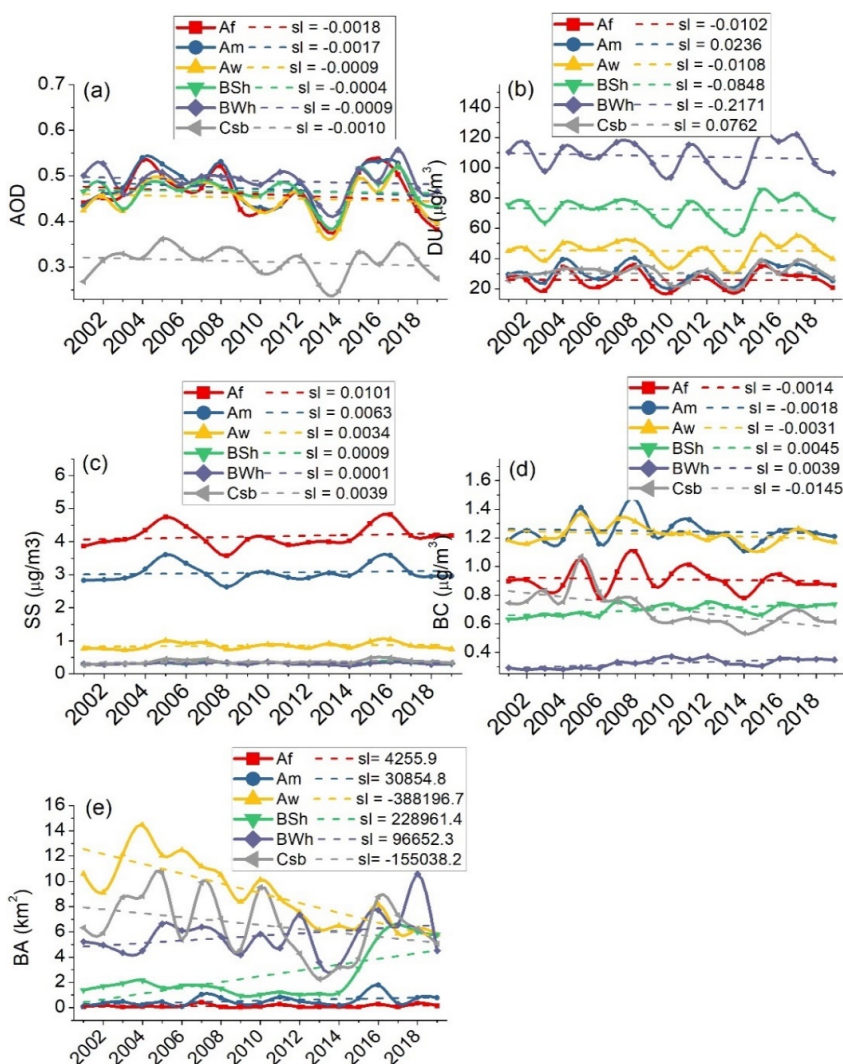


Figure 5. Annual variation of AOD, BA, and aerosol species (BC, DU, and SS) across Nigeria. The units are: AOD (unitless), BA (km^2), and aerosol species (kg/m^2).

on AOD. BA has a negligible, insignificant negative coefficient (-1.55×10^{-10} , $p = 0.71$), while DU and SS both show strong, significant positive coefficients of 5.04×10^{-3} and 9.76×10^{-2} , respectively, indicating their impact on AOD changes.

3.5. MODEL EVALUATION

The results in Figure 6 illustrate the performance of a multivariate regression model in predicting AOD across different Köppen climate zones in Nigeria, as measured by the R-squared (R^2) values. The model performs exceptionally well in the tropical monsoon (Am) and Mediterranean (Csb) zones, with high R^2 values of 0.93, indicating that it explains 93% of the variance in these regions. The tropical savanna (Aw) zone also shows strong performance, with an R^2 of 0.91. Moderate model performance is observed in the tropical rainforest (Af) and semi-arid (BSh) zones, with R^2 values of 0.84 and 0.54, respectively. However, the model struggles in the desert (BWh) zone, achieving a low R^2 of 0.22, suggesting poor predictive power in this region. These results indicate that the model is highly effective in more humid and moderate climates but less reliable in arid and desert regions,

reflecting the complexity and variability of aerosol sources and atmospheric conditions across Nigeria's diverse climatic zones.

To further validate the regression models, residual analyses were performed for each climatic zone (Figure 7). The residual plots demonstrate that the residuals are randomly distributed around zero across all fitted values, indicating that the models effectively capture the underlying trends without systematic bias. The lack of strong patterns or heteroscedasticity suggests that the assumptions of linearity and homoscedasticity are reasonably satisfied.

4. DISCUSSION

4.1. TEMPORAL TRENDS OF AEROSOL COMPONENTS

Long-term changes in aerosol properties across Nigeria's Köppen climate zones reveal that both seasonal processes and large-scale atmospheric dynamics influence aerosol behavior. Rather than focusing on isolated peaks, the overall temporal pattern indicates periodic changes in AOD corresponding to years of increased dust transport, biomass burning activity, and shifts in monsoonal circulation. These multi-year oscillations are partic-

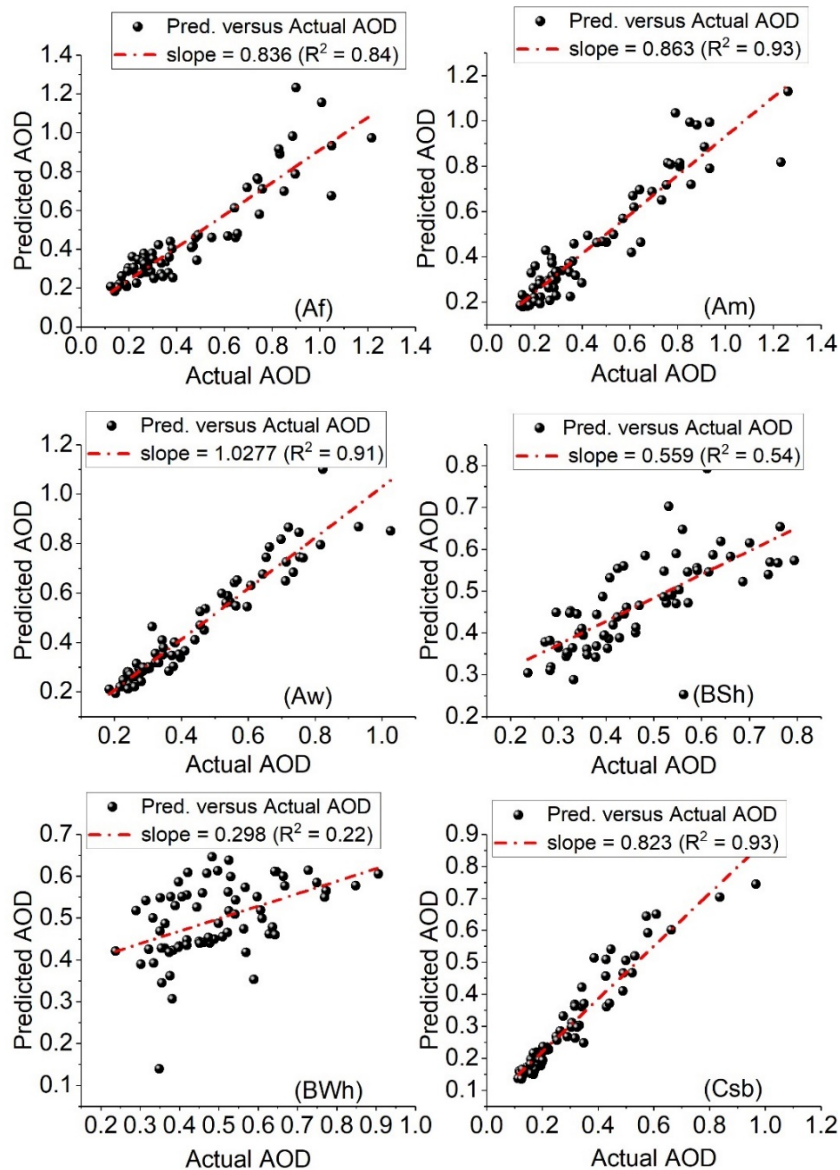


Figure 6. Multivariate regression model performance across Nigeria's climate zones based on the coefficient of determination (R^2).

ularly evident in dust aerosols, whose variability reflects emissions from the Sahara and the Bodélé Depression, consistent with earlier observations of high dust deposition rates in northern Nigeria reported by McTainsh [26].

SS increases are associated with periods of enhanced marine influx, while BC fluctuations correspond to variations in anthropogenic combustion sources. The burned area (BA) exhibits distinct cycles characteristic of the regional fire regime. These temporal trends align with observations by Aklesso *et al.* [27], who identified similar aerosol optical depth (AOD) oscillations over West Africa.

4.2. SEASONAL AND ZONAL VARIATIONS

Seasonal changes explain the significance of atmospheric circulation in influencing aerosol dispersal over Nigeria. In the southern Af and Am zones, AOD and DU uplift peak early in the year during the dry season and decrease as rainfall intensifies,

facilitating effective wet aerosol deposition. Conversely, the Aw, BSh, and BWh zones exhibit pronounced effects of the Harmattan season, with dust-laden northeasterly winds increasing AOD and DU before declining mid-year.

Sea salt concentrations increase during periods of intense monsoon activity, while BC persists primarily throughout the dry season due to increased burning and reduced atmospheric cleansing. Burned area activity aligns with the typical December-January fire season. These patterns correspond with the influences of the Intertropical Convergence Zone (ITCZ), Harmattan winds, and maritime inflow, as described by Engelstaedter *et al.* [28] and supported by Ayanlade *et al.* [13], who identified seasonal ITCZ movement as a key driver of aerosol distribution in Nigeria.

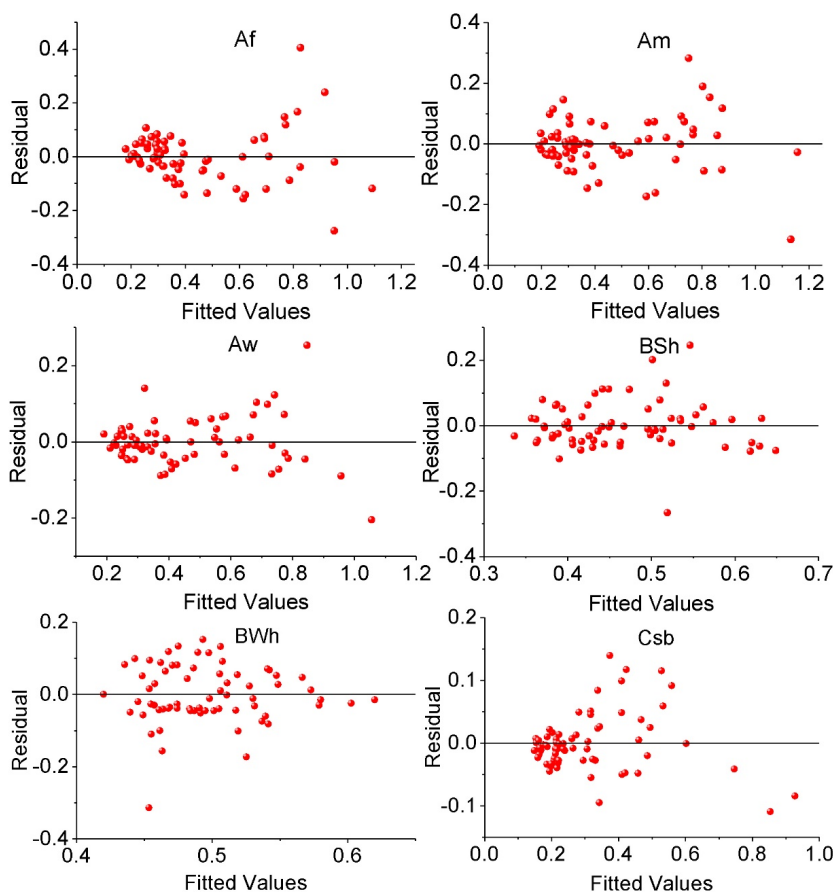


Figure 7. Multivariate regression model performance across Nigeria's climate zones based on the residual plots versus fitted values of AOD.

4.3. MULTIVARIATE REGRESSION ANALYSIS

The regression study demonstrates how the impact of various aerosol sources on AOD varies across Nigeria's climatic zones. Although BC and SS generally show positive correlations with AOD, the strength of these relationships differs by region. In some zones, BC exhibits weaker or even negative associations with AOD, suggesting interactions with more optically dominant aerosols such as dust or the moderating effects of rainy seasons.

DU consistently emerges as a significant contributor to AOD across all climatic zones, underscoring its role as a key driver of aerosol loading in Nigeria. This strong DU-AOD relationship aligns with previous regional studies that emphasize the influence of Saharan dust on West African atmospheric conditions [29–31].

Burned areas typically exhibit mixed or weak correlations with AOD, indicating that fire emissions interact with atmospheric processes such as rainfall, humidity, and dust mixing. This aligns with the findings of Yakubu and Chelty [32], who demonstrated that although biomass burning increases AOD, the direct effect varies depending on environmental factors. Generally, the regression results suggest that the impact of aerosol components on AOD depends on the climatic zone, aerosol mixing states, and seasonal meteorological conditions.

4.4. COMPLEX INTERACTIONS AND IMPLICATIONS

The presence of negative BC–AOD or BA–AOD relationships in several regions underscores the complexity of aerosol interactions in Nigeria's atmosphere. Although BC is a strong light-absorbing aerosol and a tracer for gas flaring [33], it does not always increase AOD proportionally when mixed with scattering aerosols such as dust and sea salt. The dominance of dust in northern regions can mask or dilute the optical effects of BC, while in southern regions, rainfall during the wet season enhances aerosol scavenging, thereby reducing the apparent contribution of biomass burning [34, 35].

These interactions explain why BC and BA exhibit inconsistent patterns across different climate zones. Meanwhile, the persistent positive relationship between DU and AOD across all regions aligns with Provençal *et al.* [36] and reflects the long-range transport and optical dominance of dust over other aerosol types. This study extends previous findings by demonstrating how these relationships manifest within the specific climatic contexts of Nigeria's diverse zones.

4.5. REGIONAL CONTEXT AND BROADER PERSPECTIVES

The majority of the findings support Nigeria's position at the intersection of vital natural and anthropogenic aerosol processes. High AOD values in the southern Af and Am climate zones are linked to dust incursions transported southward by the northeast trade winds, consistent with reports by McTainsh [26], Koren *et*

Table 2. Multivariate regression analysis (* for $p < 0.05$, ** for $p < 0.001$, and * for $p < 0.0001$).**

Koppen	Coefficients:	Estimate	Std. Error	P-value	Significance
Af	(Intercept)	-2.20E-02	4.94E-02	0.6566	
	BC	5.29E-02	1.82E-02	0.0042	**
	BA	2.64E-08	2.40E-08	0.2727	
	DU	7.79E-03	3.19E-04	0.0000	***
	SS	5.54E-02	9.93E-03	0.0000	***
Am	(Intercept)	-5.00E-02	4.38E-02	0.2554	
	BC	6.25E-02	1.58E-02	0.0001	***
	BA	-8.84E-09	5.82E-09	0.1309	
	DU	7.40E-03	2.68E-04	0.0000	***
	SS	7.41E-02	1.10E-02	0.0000	***
Aw	(Intercept)	1.43E-01	2.57E-02	0.0000	***
	BC	-5.33E-02	2.26E-02	0.0197	*
	BA	1.94E-10	5.18E-10	0.7086	
	DU	5.58E-03	1.59E-04	0.0000	***
	SS	1.47E-01	1.55E-02	0.0000	***
BSh	(Intercept)	1.48E-01	8.68E-02	0.0911	.
	BC	4.70E-02	1.13E-01	0.6788	
	BA	-6.92E-09	1.71E-09	0.0000	***
	DU	2.21E-03	3.25E-04	0.0000	***
	SS	4.46E-01	1.15E-01	0.0001	***
BWh	(Intercept)	3.88E-01	6.39E-02	0.0000	***
	BC	4.26E-02	1.23E-01	0.7289	
	BA	-3.76E-09	9.55E-10	0.0001	***
	DU	1.06E-03	2.50E-04	0.0000	***
	SS	-1.45E-02	9.80E-02	0.8828	
Csb	(Intercept)	9.20E-02	7.34E-03	0.0000	***
	BC	4.68E-02	8.60E-03	0.0000	***
	BA	-1.55E-10	4.15E-10	0.7100	
	DU	5.04E-03	1.70E-04	0.0000	***
	SS	9.76E-02	1.95E-02	0.0000	***

al. [37], and Li *et al.* [38]. Emissions from the Bodélé Depression significantly amplify DU levels across much of the country. Ayanlade *et al.* [13] and Onyeuwaoma *et al.* [39] have emphasized that anthropogenic sources, such as biomass burning, industrial activities, and vehicular emissions, contribute to aerosol complexity.

The spatial and temporal variations observed across climate zones demonstrate the need for region-specific monitoring approaches. The interactions among DU, BC, SS, and wildfire aerosols indicate that air quality in Nigeria is influenced by a combination of local emissions, long-range transport, and climate-dependent processes. These findings provide a stronger scientific foundation for developing zone-specific pollution control measures and policy initiatives.

5. CONCLUSION

This study reveals that the correlations between AOD and its primary influencing factors vary significantly across Nigeria's climatic zones. Dust aerosol (DU) generally has the strongest positive impact on AOD, demonstrating its crucial role in determining air visibility and radiative properties throughout the country. This finding aligns with the well-documented contribution of Saharan and Bodélé dust transport to aerosol loading in West Africa.

The effect of black carbon (BC) is more variable, as it increases AOD in humid southern zones but has negative or inconsistent effects in middle and northern zones where dust and seasonal rains modify its optical properties. Burned area (BA) contributes to aerosol loading but has varying impacts on AOD,

reflecting complex interactions with rainfall, aerosol mixing, and fire intensity. Sea salt (SS) significantly increases AOD in coastal and transitional zones, confirming the maritime influence on aerosol composition.

In conclusion, our findings emphasize the importance of considering climate-zone-specific processes when analyzing aerosol behavior in Nigeria. By incorporating various aerosol types, the study offers a more comprehensive understanding of how their interactions vary across biological and climatic gradients. This enhanced knowledge can inform more targeted air quality monitoring and the development of locally tailored strategies to regulate and mitigate aerosol-related impacts.

6. DATA AVAILABILITY

The data used in this study are publicly available and were obtained from the Climate Data Store (DOI: <https://doi.org/10.24381/cds.f333cf85>) and the Modern-Era Retrospective Analysis for Research and Applications, Version 2 (MERRA-2), provided by NASA's Global Modeling and Assimilation Office (GMAO), with the following DOIs: <https://doi.org/10.5067/FH9A0MLJPC7N> and <https://doi.org/10.5067/XOGBNQEPLUC5>.

References

- [1] H. Liao & W. Chang, "Integrated assessment of air quality and climate change for policy-making: highlights of IPCC AR5 and research challenges", *National Science Review* **1** (2014) 176. <https://doi.org/10.1093/NSR%2FNWU005>.
- [2] C. Black, Y. Tesfaigzi, J. A. Bassein & L. A. Miller, "Wildfire smoke exposure and human health: Significant gaps in research for a growing public health issue", *Environmental toxicology and pharmacology* **55** (2017) 186. <https://doi.org/10.1016/j.etap.2017.08.022>.
- [3] V. A. Ginzburg, M. S. Zelenova, V. N. Korotkov, "Estimated black carbon emissions from priority source categories in Russia", *Russian Meteorology and Hydrology* **47** (2022) 781. <https://doi.org/10.3103/S1068373922100065>.
- [4] S. Kang, Y. Zhang, P. Chen, J. Guo, Q. Zhang, Z. Cong, S. Kaspari, L. Tripathee, T. Gao, H. Niu, X. Zhong, X. Chen, Z. Hu, X. Li, Y. Li, B. Neupane, F. Yan, D. Rupakheti, C. Gul, W. Zhang, G. Wu, L. Yang, Z. Wang & C. Li, "Black carbon and organic carbon dataset over the Third Pole", *Earth System Science Data* **14** (2022) 683. <https://doi.org/10.5194/essd-14-683-2022>.
- [5] S. P. Urbanski, "Combustion efficiency and emission factors for wildfire-season fires in mixed conifer forests of the northern Rocky Mountains, US", *Atmospheric Chemistry and Physics* **13** (2013) 724. <https://doi.org/10.5194/acp-13-7241-2013>.
- [6] L. Kirago, O. Gustafsson, S. M. Gaita, S. L. Haslett, H. L. Dewitt, J. Gasore, K. E. Potter, R. G. Prinn, M. Rupakheti, J. D. Ndikubwimana, B. Safari & A. Andersson, "Atmospheric black carbon loadings and sources over Eastern Sub-Saharan Africa are governed by the regional savanna fires", *Environmental Science & Technology* **56** (2022) 15460. <https://doi.org/10.1021/acs.est.2c05837>.
- [7] R. Ramo, E. Roteta, I. Bistinas, D. van Wees, A. Bastarrika, E. Chuvieco & G. R. van der Werf, "African burned area and fire carbon emissions are strongly impacted by small fires undetected by coarse resolution satellite data", *Proceedings of the National Academy of Sciences* **118** (2021) e2011160118. <https://doi.org/10.1073/pnas.2011160118>.
- [8] S. V. Kostrykin, A. Revokatova, A. Chernenkov, V. A. Ginzburg, P. D. Polumieva & M. A. Zelenova, "Black carbon emissions from the Siberian fires 2019: Modelling of the atmospheric transport and possible impact on the radiation balance in the Arctic region", *Atmosphere* **12** (2021) 814. <https://doi.org/10.3390/atmos12070814>.
- [9] E. M. Volodin, E. V. Mortikov, S. V. Kostrykin, V. Y. Galin, V. N. Lykossov, A. S. Gritsun & N. G. Iakovlev, "Simulation of the present-day climate with the climate model INMCM5", *Climate Dynamics* **49** (2017) 3715. <https://doi.org/10.1007/s00382-016-3189-y>.
- [10] I. B. Kononov, D. A. Lvova, M. Beekmann, H. Jethva, E. F. Mikhailov, J.

- D. Paris, B. D. Belan, V. S. Kozlov, P. Ciais & M. O. Andreae, "Estimation of black carbon emissions from Siberian fires using satellite observations of absorption and extinction optical depths", *Atmospheric Chemistry and Physics* **18** (2018) 14889. <https://doi.org/10.5194/acp-18-14889-2018>.
- [11] N. Yusuf & R. S. Sa'id, "Spatial distribution of aerosols burden and evaluation of changes in aerosol optical depth using multi-approach observations in tropical region", *Heliyon* **8** (2023) e18815. <https://doi.org/10.1016/j.heliyon.2023.e18815>.
- [12] L. Menut, C. Flamant, S. Turquety, A. Deroubaix, P. Chazette & R. Meynadier, "Impact of biomass burning on pollutant surface concentrations in megacities of the Gulf of Guinea", *Atmospheric Chemistry and Physics* **18** (2018) 2687. <https://doi.org/10.5194/acp-18-2687-2018>.
- [13] A. Ayanlade, G. Atai & M. O. Jegede, "Spatial and seasonal variations in atmospheric aerosols over Nigeria: Assessment of influence of intertropical discontinuity movement", *Journal of Ocean and Climate* **9** (2019) 1. <https://doi.org/10.1177/175931311882030>.
- [14] G. Atai, A. Ayanlade, I. A. Oluwatimilehin & O. S. Ayanlade, "Geospatial distribution and projection of aerosol over Sub-Saharan Africa: assessment from remote sensing and other platforms", *Aerosol Science and Engineering* **5** (2021) 357. <https://doi.org/10.1007/s41810-021-00107-4>.
- [15] Y. A. Aliyu & J. O. Botai, "Appraising the effects of atmospheric aerosols and ground particulates concentrations on GPS-derived PWV estimates", *Atmospheric Environment* **193** (2018) 24. <https://doi.org/10.1016/j.atmosenv.2018.09.001>.
- [16] A. Ayanlade, G. Atai & M. O. Jegede, "Variability in atmospheric aerosols and effects of humidity, wind and intertropical discontinuity over different ecological zones in Nigeria", *Atmospheric Environment* **201** (2019) 369. <https://doi.org/10.1016/j.atmosenv.2018.12.039>.
- [17] N. Yusuf & R. S. Sa'id, "Spatial distribution of aerosols burden and evaluation of changes in aerosol optical depth using multi-approach observations in tropical region", *Heliyon* **9** (2023) e18815. <https://doi.org/10.1016/j.heliyon.2023.e18815>.
- [18] O. C. Ibe, O. K. Nwofor & U. K. Okoro, "Aerosol loading in the Guinea Coast climate region of Nigeria: comparison of MODIS and AERONET data sources", *Discover Atmosphere* **2** (2024) 14. <https://doi.org/10.1007/s44292-024-00018-2>.
- [19] Copernicus Climate Change Service, "Fire burned area from 2001 to 2019 (Version 3.1) [Burned area]", *Climate Data Store* (2020). <https://doi.org/10.24381/cds.f333cf85>.
- [20] Global Modeling and Assimilation Office (GMAO), "instM_2d_gas_Nx: MERRA-2 2D, diurnal, instantaneous, single-level, assimilated aerosol optical depth analysis (0.625x0.5), version 5.12.4.", Greenbelt, MD, USA: Goddard Space Flight Center Distributed Active Archive Center (GSFC DAAC), 2023. <https://doi.org/10.5067/XOGNBQEPLUC5>.
- [21] Global Modeling and Assimilation Office (GMAO), "tavM_2d_aer_Nx: MERRA-2 2D, monthly mean, time-averaged, single-level, assimilated aerosol diagnostics (0.625x0.5), version 5.12.4.", Greenbelt, MD, USA: Goddard Space Flight Center Distributed Active Archive Center (GSFC DAAC), 2023. <https://doi.org/10.5067/FH9A0MLJPC7N>.
- [22] H. E. Beck, T. R. McVicar, N. Vergopolan, A. Berg, N. J. Lutsko, A. Dufour, Z. Zeng, X. Jiang, A. I. J. M. van Dijk & D. G. Miralles, "High-resolution (1 km) Köppen-Geiger maps for 1901–2099 based on constrained CMIP6 projections", *Scientific Data* **10** (2023) 724. <https://doi.org/10.1038/s41597-023-02549-6>.
- [23] D. Stockemer, "Multivariate regression analysis", in *Quantitative methods for the social sciences*, D. Stockemer (Ed.), Springer, Cham, Switzerland, 2019, pp. 129–142. https://doi.org/10.1007/978-3-319-99118-4_9.
- [24] A. J. Duleba & D. L. Olive, "Regression analysis and multivariate analysis", *Seminars in Reproductive Endocrinology* **14** (1996) 139. <https://doi.org/10.1055/s-2007-1012915>.
- [25] A. C. Cameron & F. A. G. Windmeijer, "An R-squared measure of goodness of fit for some common nonlinear regression models", *Journal of Econometrics* **77** (1997) 329. [https://doi.org/10.1016/S0304-4076\(96\)01818-0](https://doi.org/10.1016/S0304-4076(96)01818-0).
- [26] G. McTainsh, "Harmattan dust deposition in Northern Nigeria", *Nature* **286** (1980) 587. <https://doi.org/10.1038/286587a0>.
- [27] M. Aklesso, K. R. Kumar, L. Bu & R. Boiyo, "Analysis of spatial-temporal heterogeneity in remotely sensed aerosol properties observed during 2005–2015 over three countries along the Gulf of Guinea Coast in Southern West Africa", *Atmospheric Environment* **182** (2018) 313. <https://doi.org/10.1016/j.atmosenv.2018.03.062>.
- [28] S. Engelstaedter, I. Tegen & R. Washington, "North African dust emissions and transport", *Earth-Science Reviews* **79** (2006) 73. <https://doi.org/10.1016/j.earscirev.2006.04.002>.
- [29] A. Konare, A. S. Zakey, F. Solmon, F. Giorgi, S. Rauscher, S. Ibrah & X. J. J. Bi, "A regional climate modeling study of the effect of desert dust on the West African monsoon", *Journal of Geophysical Research: Atmospheres* **113** (2008) D12. <https://doi.org/10.1029/2007JD009322>.
- [30] K. B. Raji, K. O. Ogunjobi & A. A. Akinsanola, "Radiative effects of dust aerosol on West African climate using simulations from RegCM4", *Modeling Earth Systems and Environment* **3** (2017) 34. <https://doi.org/10.1007/s40808-017-0295-y>.
- [31] E. T. N'Datchoh, I. Diallo, A. Konaré, S. Silué, K. O. Ogunjobi, A. Diedhiou & M. Doumbia, "Dust induced changes on the West African summer monsoon features", *International Journal of Climatology* **38** (2018) 452. <https://doi.org/10.1002/joc.5187>.
- [32] A. T. Yakubu & N. Chetty, "Optical properties of atmospheric aerosol over Cape Town, Western Cape of South Africa: Role of biomass burning", *Atmosfera* **34** (2021) 395. <https://doi.org/10.20937/atm.52811>.
- [33] O. G. Fawole, X. Cai, J. G. Levine, R. T. Pinker & A. R. MacKenzie, "Detection of a gas flaring signature in the AERONET optical properties of aerosols at a tropical station in West Africa", *Journal of Geophysical Research: Atmospheres* **121** (2016) 14512. <https://doi.org/10.1002/2016JD025584>.
- [34] Y. Wang, W. Xia, X. Liu et al., "Disproportionate control on aerosol burden by light rain", *Nature Geoscience* **14** (2021) 72. <https://doi.org/10.1038/s41561-020-00675-z>.
- [35] H. Jeoung, C. E. Chung, T. Van Noije & T. Takemura, "Relationship between fine-mode AOD and precipitation on seasonal and interannual time scales", *Tellus B: Chemical and Physical Meteorology* **66** (2014) 23037. <https://doi.org/10.3402/tellusb.v66.23037>.
- [36] S. Provençal, P. Kishcha, A. M. da Silva, E. Elhacham & P. Alpert, "AOD distributions and trends of major aerosol species over a selection of the world's most populated cities based on the 1st version of NASA's MERRA Aerosol Reanalysis", *Urban Climate* **20** (2017) 168. <http://dx.doi.org/10.1016/j.uclim.2017.04.001>.
- [37] I. Koren, Y. J. Kaufman, R. Washington, M. C. Todd, Y. Rudich, J. V. Martins & D. Rosenfeld, "The Bodélé depression: a single spot in the Sahara that provides most of the mineral dust to the Amazon forest", *Environmental Research Letters* **1** (2006) 1. <https://doi.org/10.1088/1748-9326/1/1/014005>.
- [38] B. Li, S. Su, H. Yuan & S. Tao, "Spatial and temporal variations of AOD over land at the global scale", *International Journal of Remote Sensing* **33** (2012) 2097. <https://doi.org/10.1080/01431161.2011.605088>.
- [39] N. D. Onyeuwaoma, O. K. Nwofor, T. C. Chineke, E. O. Eguaroje & V. N. Dike, "Implications of MODIS impression of aerosol loading over urban and rural settlements in Nigeria: Possible links to energy consumption patterns in the country", *Atmospheric Pollution Research* **6** (2015) 484. <https://doi.org/10.5094/apr.2015.054>.